BBA - Bioenergetics 1860 (2019) 452–460

Contents lists available at ScienceDirect

BBA - Bioenergetics

journal homepage: www.elsevier.com/locate/bbabio

Fourier transform visible and infrared difference spectroscopy for the study of P700 in photosystem I from *Fischerella thermalis* PCC 7521 cells grown under white light and far-red light: Evidence that the A_{-1} cofactor is chlorophyll *f*

Gary Hastings[a,*], Hiroki Makita[a], Neva Agarwala[a], Leyla Rohani[a], Gaozhong Shen[b], Donald A. Bryant[b,c]

[a] Department of Physics and Astronomy, Georgia State University, Atlanta, GA, USA
[b] Department of Biochemistry and Molecular Biology, The Pennsylvania State University, University Park, PA, USA
[c] Department of Chemistry and Biochemistry, Montana State University, Bozeman, MT, USA

ARTICLE INFO

Keywords:
Photosynthesis
Cyanobacteria
FTIR
Photosystem I
P700
Chlorophyll *f*
FaRLiP

ABSTRACT

($P700^+$ – P700) Fourier transform visible and infrared difference spectra (DS) have been obtained using photosystem I (PSI) complexes isolated from cells of *Fischerella thermalis* PCC 7521 grown under white light (WL) or far-red light (FRL). PSI from cells grown under FRL (FRL-PSI) contain ~8 chlorophyll *f* (Chl *f*) molecules (Shen et al., *Photosynth. Res.* Jan. 2019). Both the visible and infrared DS indicate that neither the P_A or P_B pigments of P700 are Chl *f* molecules, but do support the conclusion that at least one of the A_{-1} cofactors is a Chl *f* molecule.

The FTIR DS indicate that the hydrogen bond to the 13^1-keto C=O group of the P_A pigment of P700 is weakened in FRL-PSI, as might be expected given that the proteins that bind the P700 pigments are substantially different in FRL-PSI (Gan et al., *Science* 345, 1312–1317, 2014).

The FTIR DS obtained using FRL-PSI display a band at 1664 cm^{-1} that is assigned (based on density functional theory calculations) to the 2^1-formyl C=O group of Chl *f*, that upshifts 5 cm^{-1} upon $P700^+$ formation. This is much less than expected for a cation-induced upshift, indicating that the Chl *f* molecule is not one of the pigments of P700.

In WL-PSI the A_{-1} cofactor is a Chl *a* molecule with 13^1-keto and 13^3-methylester C=O mode vibrations at 1696 and 1750 cm^{-1}, respectively. In FRL-PSI the A_{-1} cofactor is a Chl *f* molecule with 13^1-keto and 13^3-methylester C=O mode vibrations at 1702 and 1754 cm^{-1}, respectively.

1. Introduction

In photosynthesis, light drives a set of reactions that result in products essential for the maintenance of life on Earth. In oxygen-evolving organisms two photosystems, called photosystems one and two (PSI and PSII)[1] capture and convert solar energy independently but cooperatively [1]. The solar conversion reactions occur in a central pigment-protein complex called a reaction center (RC). In the RC, light is used to drive electrons vectorially, via a series of acceptors, across a biological membrane [1].

PSI uses light to catalyze the formation of strong reductants that are used to assimilate carbon dioxide into complex organic molecules [2]. In cyanobacteria, PSI consists of 11–12 protein subunits, many of which have been characterized [3]. Most of the electron transfer (ET) cofactors are bound to the PsaA and PsaB membrane-spanning proteins. The terminal ET acceptors, F_A and F_B, are bound to the stromal, membrane-extrinsic PsaC subunit [3]. Fig. 1A shows the two nearly symmetrical branches of ET cofactors found in PSI. The branches are labeled A and B according to whether the A_1 quinone cofactor is bound to PsaA or PsaB. Fig. 1A is generated using the 2.5 Å X-ray crystal structure of trimeric

* Corresponding author.
E-mail address: ghastings@gsu.edu (G. Hastings).

[1] Abbreviations: Chl *a*, chlorophyll *a*; Chl *f*, chlorophyll *f*; DFT, density functional theory; DM, *n*-dodecyl-β-D-maltoside; DS, difference spectra/spectrum/spectroscopy; DDS, double difference spectrum; ET, electron transfer; FaRLiP, far-red light photoacclimation; FRL, far red light; *F.*, *Fischerella*; FTIR, Fourier transform infrared; H-bond, hydrogen bond; LT, low temperature (~77 K); μs/ms/ns, micro/milli/nano-second; PSI, photosystem one; RCs, reaction centers; RT, room temperature (~298 K); *S6803*, *Synechocystis* sp. PCC 6803; T., *Thermosynechococcus*. WL, white light.

https://doi.org/10.1016/j.bbabio.2019.04.002
Received 23 February 2018; Received in revised form 20 December 2018; Accepted 6 January 2019
Available online 13 April 2019

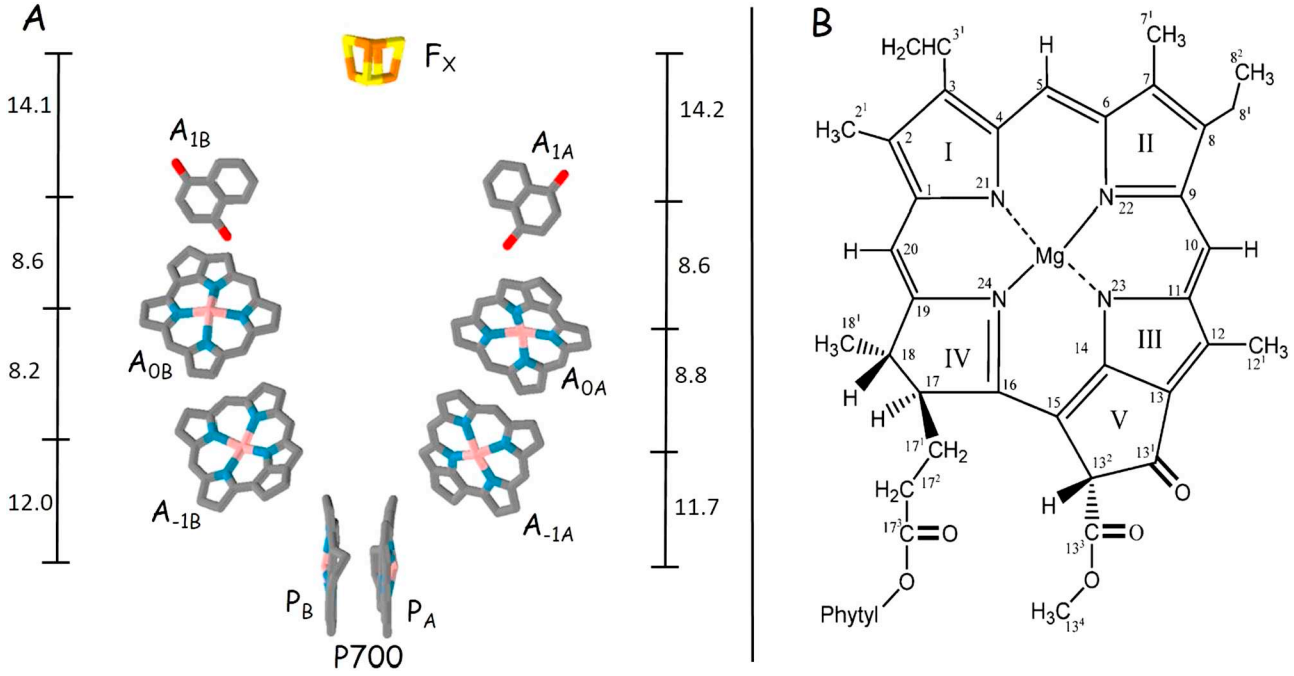

Fig. 1. (A) Schematic of the ET cofactor chains in PS I. Center to center distances between the cofactors (in Å) are indicated (taken from [4]). No antenna Chl *a* pigment is within ~18 Å (Mg…Mg distance) of either P_B or P_A [4]. (B) Structure and IUPAC numbering scheme for chlorophyll *a* (Chl *a*). The C═O functional groups at the 17^3, 13^3 and 13^1 positions contribute prominently in FTIR DS. Chl *a′* is a 13^2 epimer of Chl *a*. Chl *f* has a formyl group instead of a methyl group at the 2-position.

PSI complexes from the cyanobacterium *Thermosynechococcus elongatus* (*T. elongatus*) (PDB file accession number 1JB0) [4].

In PSI light excitation results in a series of ET processes, that within a few hundred nanoseconds have led to formation of the $P700^+F_{A/B}^-$ radical-pair state [5]. We use the subscript A/B to indicate that we do not specifically distinguish between F_A and F_B. In isolated PSI complexes, the $P700^+F_{A/B}^-$ radical-pair state has a lifetime of 40–80 ms [5,6]. Because the $P700^+F_{A/B}^-$ state is so long-lived, it is straightforward to photo-accumulate a large population of this state, and ($P700^+F_{A/B}^-$ – $P700F_{A/B}$) FTIR DS are easily produced [7]. ($P700^+F_{A/B}^-$ – $P700F_{A/B}$) FTIR DS are usually produced in the 2000–1000 cm^{-1} spectral region. Iron-sulfur clusters do not absorb in this spectral region, and we simply refer to the DS as ($P700^+$ – P700) FTIR DS [7–9]. It is also possible to collect DS for samples under identical conditions, but using visible/near-infrared probing light in the ~680–1000 nm range [10], which we call ($P700^+$ – P700) FT-visible DS.

To understand the origin of bands in ($P700^+$ – P700) FTIR DS, experiments have been undertaken for PSI particles under a myriad of conditions, from site-directed mutants that impact the P700 pigments [11,12], to global [13] and specific [14] isotopic labeling of the PSI particles. Several comprehensive reviews of work undertaken to understand the nature of the bands in ($P700^+$ – P700) FTIR DS have appeared in the literature, the most recent being in 2006 [7].

The structure of Chl *a* is shown in Fig. 1B. It is a magnesium-containing, pentacylic porphyrin, with a phytol tail esterified to the propionate moiety at the C17 position. Chl *a* contains a vinyl group at position 3 and three carbonyl groups at the 13^1, 13^3 and 17^3 positions. Chl *a′* is a 13^2 epimer of Chl *a*. Chl *a* has a methyl group at the C2 position, which is replaced by a formyl group in Chl *f* [15].

The structural organization of the P_B and P_A pigments of P700 are depicted in Fig. 2. The P_A and P_B macrocycles are parallel and separated by ~3.6 Å. Pyrrole rings I and II of P_A and P_B overlap, and the central Mg^{2+} ions of P_A and P_B are separated by 6.3 Å. P_A and P_B are axially ligated to HisA680 and HisB660 (*T. elongatus* numbering scheme). Fig. 2 demonstrates that the amino acid environment surrounding P_A and P_B is decidedly asymmetric, with only P_A being involved in hydrogen bonding (H-bonding). The hydroxyl oxygen atom of ThrA743 is 2.98 Å from the 13^1-keto C═O oxygen atom of P_A and is suitably positioned to form an H-bond. In addition, the ThrA743 hydroxyl oxygen atom is 2.7 Å from the oxygen atom of a water molecule (H_2O-19). The H_2O-19 oxygen atom is 3.28 Å from the 13^3-ester oxygen atom, and is also within H-bonding distance of TyrA603 and SerA607. Thus, the C═O groups of P_A are embedded in a complex H-bond network. The C═O groups of P_B are free of any H-bonding interactions.

The P_A and P_B pigments of P700 are within 12 Å of the A_{-1A} and A_{-1B} pigments, respectively (Fig. 1B and Table S1), but more than 18 Å from the nearest antenna pigment [4]. The A_{-1} and A_0 pigments on both the A and B branches are within 12 Å of a Chl *a* antenna pigment, numbered A39 and B39 in the *T. elongatus* PSI crystal structure [4].

In recent years it has been shown that certain strains of cyanobacteria can thrive in environments enriched in FRL (700–800 nm) due to an acclimation process known as far-red light photoacclimation (FaRLiP) [16–18]. These cyanobacterial strains contain a conserved 20-gene cluster that encodes paralogous subunits for the core complexes of PSI, PSII, and phycobilisomes, as well as the Chl *f* synthase [16,17,19]. Expression of the genes in this cluster is controlled by a red/far-red responsive knotless phytochrome (RfpA), a CheY-like phosphotransferase (RfpC), and a transcriptional activator/response regulator (RfpB) [17,18]. When cells are grown in light conditions under which wavelengths longer than about 700 nm predominate, the photosynthetic apparatus is extensively modified and Chl *f* and Chl *d* are synthesized, replacing about 7–8% and 1% of the Chl *a*, respectively. Chl *d* is exclusively associated with PSII [20], but Chl *f* is found in both photosystems produced in FRL. The PsaA1, PsaB1, PsaF1, PsaI1, PsaJ1, and PsaL1 subunits of PSI are replaced with paralogs from the FaRLiP gene cluster, and similarly, the core Chl *a*-binding subunits (PsbA, PsbB, PsbC, PsbD, PsbH) of PSII are also replaced by paralogous subunits [16] Recent studies have confirmed that P700 PSI is still formed by a Chl *a*/Chl *a′* heterodimer as occurs in PSI complexes produced in WL [20–22].

Here we have studied PSI complexes from *F. thermalis* cells grown in

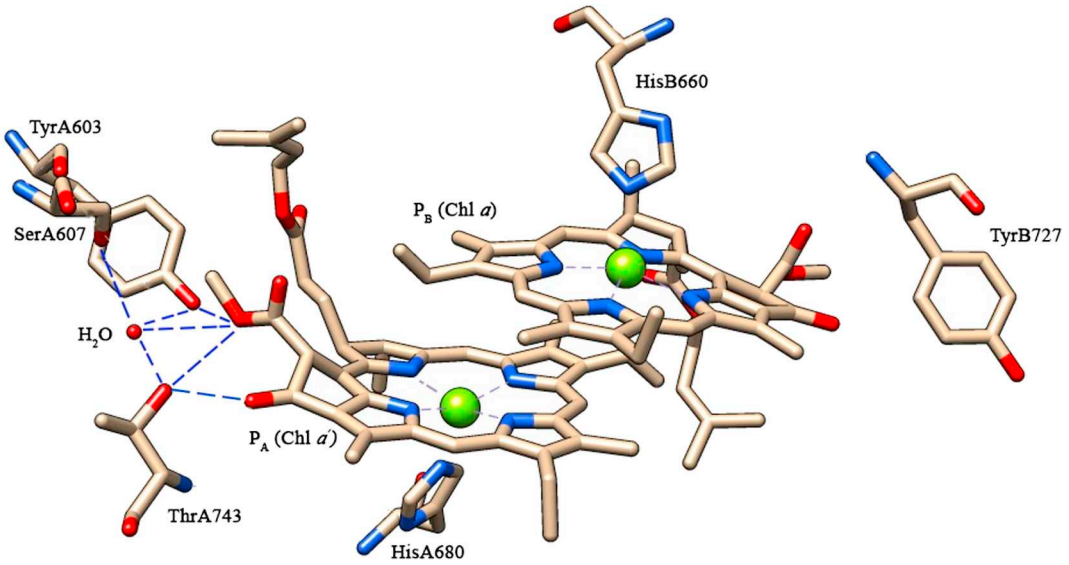

Fig. 2. Structure and protein environment surrounding the P_A and P_B pigments of P700. Possible H-bonds are indicated (*blue dotted line*). Model derived from the PSI X-ray crystal structure at 2.5 Å resolution [4].

white light (WL-PSI) or FRL (FRL-PSI) to determine whether there are changes in the chlorophyll pigments in the ET chain in the FRL-PSI complexes.

2. Materials and methods

2.1. Cell culture, growth and isolation of PSI complexes

Fischerella thermalis PCC 7521 (*F. thermalis*) was obtained from the Pasteur Culture Collection. The strain was originally isolated from a hot spring near Mammoth Sinkhole II in Yellowstone National Park, WY, USA [23]. Cells of *F. thermalis* were grown in B-HEPES medium, a modified BG11 medium containing 1.1 g/L HEPES (final concentration) with the pH adjusted to 8.0 with 2.0 M KOH [24]. Liquid cultures were sparged with 1% (v/v) CO_2 in air. Cells were grown under white light (WL) and far-red light (FRL). For WL, warm white fluorescent bulbs were used to provide continuous illumination at ~100 μmol photons $m^{-2} s^{-1}$. For FRL, LEDs (Marubeni, Santa Clara, CA) with emission centered at 720 nm were used (15–18 μmol photons $m^{-2} s^{-1}$), in combination with green and red light-transmitting filters, as described previously [19,25].

PSI complexes were purified from *F. thermalis* cells grown under WL and FRL as described previously [25,26]. Briefly, cells were harvested and resuspended in PSI isolation buffer (50 mM 2-(N-morpholino) ethanesulfonic acid (MES), pH 6.5, 10 mM CaCl2 and 10 mM MgCl2). Cell lysis was achieved using a chilled French press at 138 kPa, and at 4 °C. Thylakoid membranes prepared by ultracentrifugation were solubilized in 1% (w/v) *n*-dodecyl-β-D-maltoside (DM) with gentle stirring at 4 °C. Solubilized membranes were loaded onto 5–20% linear sucrose gradients in PSI isolation buffer containing 0.1% (w/v) DM, which were subjected to ultracentrifugation (133,900 × *g*) for about 18 h. Green bands containing trimeric PSI complexes were collected from the sucrose gradients, dialyzed against PS I isolation buffer and concentrated using the Millipore Centriprep 100 K centrifugal filter devices (EMD Millipore, Darmstadt, Germany). The concentrated PSI samples were further purified through a second ultracentrifugation under identical conditions. Green bands containing trimeric PSI particles were collected from the second sucrose gradients, dialyzed against PSI isolation buffer and concentrated as described above. Purified PSI particles were resuspended in PSI buffer (50 mM MES, pH = 6.5, 10 mM $CaCl_2$, 10 mM $MgCl_2$, 0.05% (w/v) DM and 5% (w/v) glycerol) and stored at –80 °C until use. FRL-PSI samples from *F. thermalis* contain approximately 7-8 Chl *f* and no Chl *d* molecules per 100 total Chls [25].

2.2. Spectroscopic measurements

Samples containing WL-PSI and FRL-PSI complexes were centrifuged to form a soft pellet, which was squeezed between two 1-inch diameter CaF_2 windows. Approximately 20 mM ascorbate was added. The spacing between the windows was adjusted so that the amide I absorption band had an OD = ~0.8 units. In the visible region the same sample had a peak Q_y absorption near 680 nm that was above 3.0 in OD units, but the OD at ~700 nm was less than 0.5. Such a high OD at 680 nm makes spectral measurement at or near this wavelength nearly impossible. All experiments were performed at room temperature (RT, ~298 K).

Light-induced FTIR DS were recorded with a Bruker Vertex 80 FTIR spectrometer, equipped with a globar light source, KBr beam-splitter and liquid-nitrogen-cooled HgCdTe detector, which allows measurements in the 7000–1100 cm^{-1} spectral region. FT-visible difference spectra were recorded with a Bruker IFS66 spectrometer, equipped with a halogen lamp (GE 75 W), quartz beam-splitter and a silicon diode photodetector, allowing measurements up to the helium neon laser wavelength (632.8 nm). A 17-mW helium neon laser, expanded to a spot size of ~8 mm at the sample, was used as actinic light source in all DS measurements.

In FT-visible DS measurements the probing light impinging on the sample was filtered using three 3-mm thick 665 nm (center wavelength) long-pass filters, to eliminate actinic effects of the measuring light and to block the interferometer helium neon laser. The detector was protected from scattered 632.8 nm actinic laser light using a fourth 665 nm long-pass filter. Spectral resolution was set at 24 cm^{-1}, with a phase resolution of 48 cm^{-1} using a Mertz phase correction.

For FTIR DS the IR light impinging on the sample was filtered using a 1000–5000 cm^{-1} band-pass filter. This filter also blocks the interferometer helium-neon laser light from reaching the sample. The IR light impinging on the detector is further filtered using a second 1000–5000 cm^{-1} band-pass filter to protect the MCT detector from scattered 632.8 nm laser light.

In both FT-visible and FTIR DS measurements, 64 interferograms are collected and averaged in the dark, prior to illumination. The averaged interferogram is Fourier-transformed to produce a single-

beam spectrum (background spectrum or "dark" spectrum). A single-beam spectrum is then collected during laser illumination of the sample (64 interferograms) and the resulting spectrum is (log) ratioed against the background spectrum to produce an absorption difference spectrum (often called a "light minus dark" difference spectrum, or a ($P700^+$ – P700) DS). Further sets of single-beam spectra are collected without sample illumination until no signal due to the actinic illumination is observed in the "dark minus dark" DS. This procedure is repeated 100–300 times and the results from each set of measurements are averaged.

2.3. Vibrational frequency calculations

For density functional theory (DFT) calculations, all geometry optimizations and harmonic, normal-mode vibrational frequency calculations for neutral and oxidized Chl *a* and Chl *f* were performed using Gaussian 16 software [27]. The phytyl tail is truncated to a five carbon unit [$(CH)_2C(CH_3)_2$]. The B3LYP functional was used in combination with the 6-31G + (d) basis set. A standard frequency scaling factor was employed to bring the calculated bands into line with experiment [28,29]. Radical-induced frequency shifts and isotope-induced frequency shifts are accurately calculated without scaling, however [29].

To model solvent effects, the integral equation formalism of the polarizable continuum model was used [30–33], as it is implemented in Gaussian 16.

No negative frequencies were calculated for any of the model molecular structures discussed.

3. Results

Fig. 3 shows light-induced ($P700^+$ – P700) FT-visible DS obtained at RT in the ~690–920 nm region for WL- (*blue*) or FRL-PSI (*red*) from *F. thermalis*. Spectral resolution is ~1 nm, and peak positions are measured to an accuracy below 0.25 nm.

Fig. 4 shows light–induced ($P700^+$ – P700) FTIR DS obtained at RT in the ~1770–1530 cm^{-1} region for WL-PSI and FRL-PSI from *F. thermalis*. Spectra were collected at 4 cm^{-1} spectral resolution. Spectra collected at 2 cm^{-1} spectral resolution are shown in Fig. 5.

DFT calculated FTIR spectra for neutral Chl *a* and Chl *f*, and also for Chl f^+, in THF, in the 1680–1620 cm^{-1} region, are shown in Fig. 6.

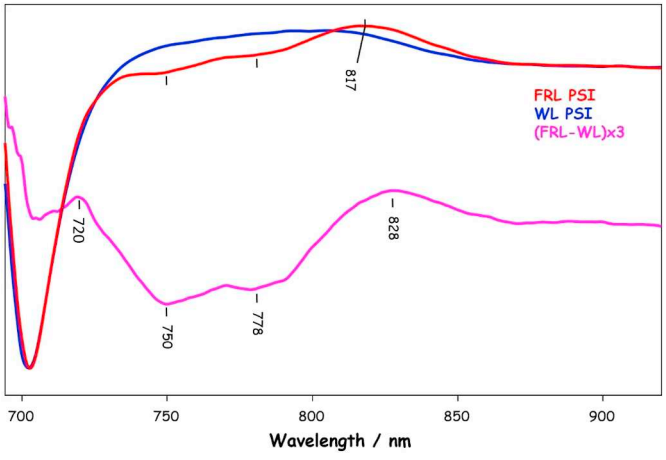

Fig. 3. Light-induced ($P700^+$ – P700) FT-visible DS obtained using isolated PSI complexes from *F. thermalis* cells grown under WL (*blue*) and FRL (*red*). The spectra were scaled to the negative band at ~702 nm. The difference between the two spectra (scaled by a factor of three) is also shown (*magenta*).

4. Discussion

4.1. ($P700^+$ – P700) FT-visible DS

The ($P700^+$ – P700) FT-visible DS in Fig. 3 for WL-PSI is similar to spectra obtained for PSI from other cyanobacterial strains [21,34]. A broad bleaching at 702.4 nm is due to the loss of P700 ground state absorption while the very broad positive absorption centered near 800 nm is due to $P700^+$ formation. ($P700^+$ – P700) FT-visible DS for PSI from cells grown under FRL (FRL-PSI) display a similar bleaching slightly red-shifted to 702.9 nm. However, FT-visible DS for the FRL-PSI and WL-PSI complexes are distinctly different beyond ~730 nm, with the FRL-PSI DS displaying weak but obvious bleaching at ~750 and ~778 nm. The FRL-PSI DS also shows a broad positive peak at 817 nm, that is probably due to $P700^+$ absorption. Additionally, the bandwidth of the difference feature between ~740–800 nm in the DDS in Fig. 3 is larger than might be expected for coupled Chl pigments. Certainly the width is much larger than the ~702 nm bleaching band.

This FRL-PSI DS in Fig. 3 is similar to that obtained for FRL-PSI samples from *Synechococcus* sp. PCC 7335 [21] for which only a single negative peak near 770 nm was observed. The differences in the spectra in Fig. 3 in the 735–800 nm range likely relate to absorption associated with one or more Chl *f* molecules that are influenced by $P700^+$ formation. These Chl *f* molecules are therefore likely to be close to the P_A and/or P_B Chls of P700.

From the observation of an intense bleaching at 702–703 nm in the DS for both FRL-PSI and WL-PSI, it is unlikely that the P_A or P_B pigments of P700 are Chl *f* molecules, which would presumably lead to an intense bleaching at wavelengths far to the red (~40 nm) of 700 nm. This has been suggested previously [20–22]. Thus, characterization of multiple FRL-PSI complexes leads to the conclusion that P700 is likely a Chl *a*/Chl *a*' heterodimer in all cyanobacterial strains that can perform FaRLiP.

4.2. WL-PSI ($P700^+$ – P700) FTIR DS

In ($P700^+$ – P700) FTIR DS (Fig. 4), positive/negative bands are associated with $P700^+$/P700, respectively. In the FTIR DS for WL-PSI positive bands are observed at 1653, 1670, 1687, 1718, 1742 and 1754 cm^{-1}, while negative bands are found at 1636, 1666, 1679, 1698, 1734 and 1748 cm^{-1}. The FTIR DS for WL-PSI is very similar to that found for PSI from other cyanobacterial strains, and many of the bands in the spectra have been assigned [7].

For example, the 1734(–)/1742(+) and 1748(−)/1754(+) cm^{-1} difference bands have been assigned to the 13^3-methylester C═O groups of the P_A and P_B pigments of P700, respectively (see Fig. 1B for Chl *a* numbering scheme). The difference band for the 13^3-methylester C═O of P_A occurs at a lower frequency due to the fact that it may be H-bonded, or at least it finds itself in the midst of a complicated H-bond network (Fig. 2). The difference features in the WL-FTIR DS indicate that the negative bands at 1734 and 1749 upshifts 8 and 6 cm^{-1} upon cation formation, respectively. Given the similarity in the up-shift, it has been suggested that the cation charge is evenly distributed or delocalized over both the P_A and P_B pigments of P700.

The intense negative band at ~1698 cm^{-1} in the WL-PSI FTIR DS is believed to be mostly due to the 13^1-keto C═O group of P_B, that upshifts 20 cm^{-1} to 1718 cm^{-1} upon cation formation. This interpretation does not provide an explanation for the splitting of this band observed in the FTIR DS obtained for PSI from mutants in which the histidine at A680, which provides and axial ligand to P_A (Fig. 2), is changed to serine [8]. This interpretation also does not provide an explanation for the origin of the positive band at 1687 cm^{-1}. Nonetheless, it is quite well accepted that at least a portion of the 1698(−) cm^{-1} band is due to the 13^1-keto C═O of P_B, that upshifts to 1718 cm^{-1} upon cation formation.

In the WL-PSI FTIR DS the difference band at 1636(−)/1653(+)

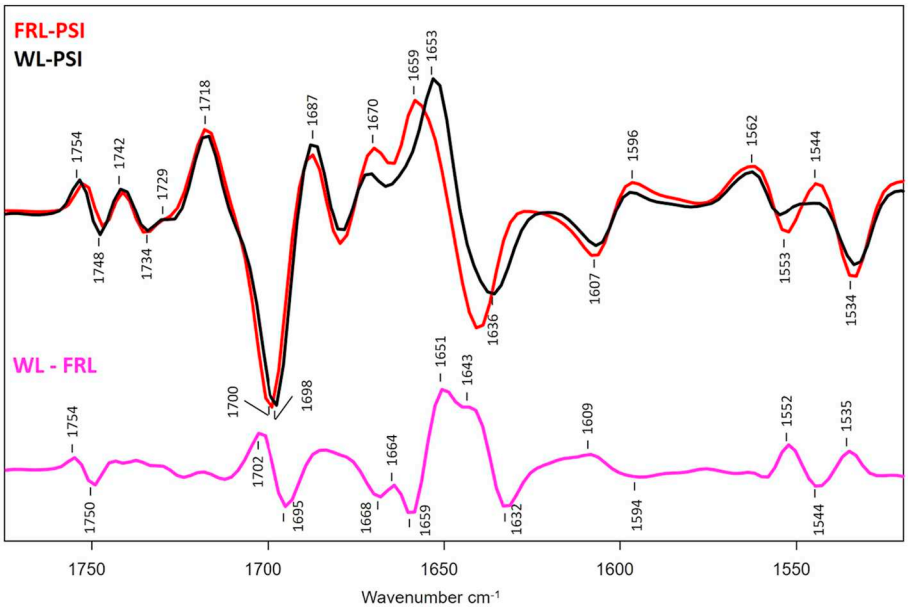

Fig. 4. ($P700^+$ – P700) light-induced FTIR DS obtained using FRL-PSI (*red*) and WL-PSI (*black*) particles from *F. thermalis*. The spectra were scaled in a way that minimizes the differences in the signals in the ~1680–1760 cm^{-1} region. A double difference spectrum (DDS) obtained by subtracting the spectra for FRL-PSI from WL-PSI is also shown (*magenta*). Spectral resolution is 4 cm^{-1}.

cm^{-1} has been assigned to the 13^1-keto C=O group of P_A/P_A^+, respectively. Thus the 13^1-keto C=O group of P_A/P_A^+ is downshifted nearly 60 cm^{-1} compared to P_B/P_B^+, indicating that the 13^1-keto C=O of both P_A and P_A^+ is very strongly H-bonded [35]. This assignment is in agreement with analysis based on the X-ray crystal structure (Fig. 2), and with FTIR DS studies of mutant PSI particles in which the H-bonding ThrA743 residue is changed to a non-H-bonding residue [36,37].

Furthermore, the 1636(−)/1653(+) cm^{-1} difference band suggests an upshift of 17 cm^{-1} for the 13^1 keto C=O mode of P_A upon cation formation, similar to that for the 13^1 keto C=O mode of P_B. As suggested above for the 13^3-methylester C=O groups, given the similarity in the cation induced upshift of the 13^1 keto C=O modes of P_A and P_B, as well as the intensity of the difference bands, it has been suggested that the cation charge is evenly distributed or delocalized over both the P_A and P_B pigments of P700 [35]. This conclusion is not in agreement with conclusions drawn from EPR measurements, however, which indicate the charge is predominantly localized on the P_B pigment [38].

The molecular groups that give rise to the bands in the spectra in Fig. 3 for WL-PSI are summarized in Table 1.

4.3. FRL-PSI ($P700^+$ - P700) FTIR DS

The FTIR DS for FRL-PSI and WL-PSI display several differences, the most obvious being that the 1636(−)/1653(+) cm^{-1} difference band is upshifted ~7 cm^{-1} in the FRL-PSI DS. The 1718(+) cm^{-1} difference band is at the same position for both WL-PSI and FRL-PSI. The 1698(−) cm^{-1} band in the WL-PSI FTIR DS is downshifted 2 cm^{-1} compared to the corresponding band in the FRL-PSI FTIR DS. Given this downshift it is interesting to note that the 1748(−)/1754(+) cm^{-1} difference band

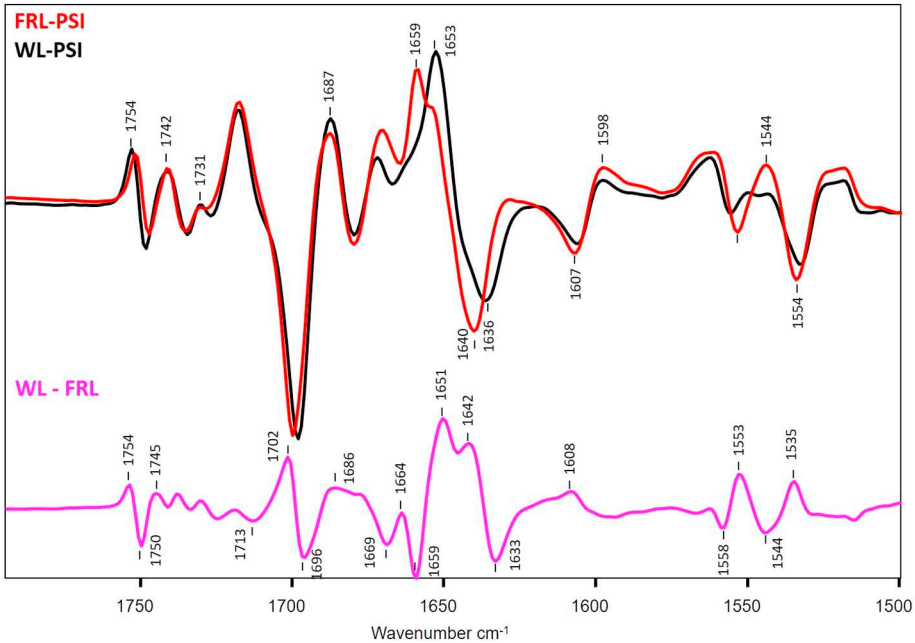

Fig. 5. The same spectra as in Fig. 4, but collected at 2-cm^{-1} spectral resolution. ($P700^+$ − P700) FTIR DS obtained using WL-PSI (*black*) and FRL-PSI (*red*) samples. The (WL – FRL) DDS is also shown (*magenta*).

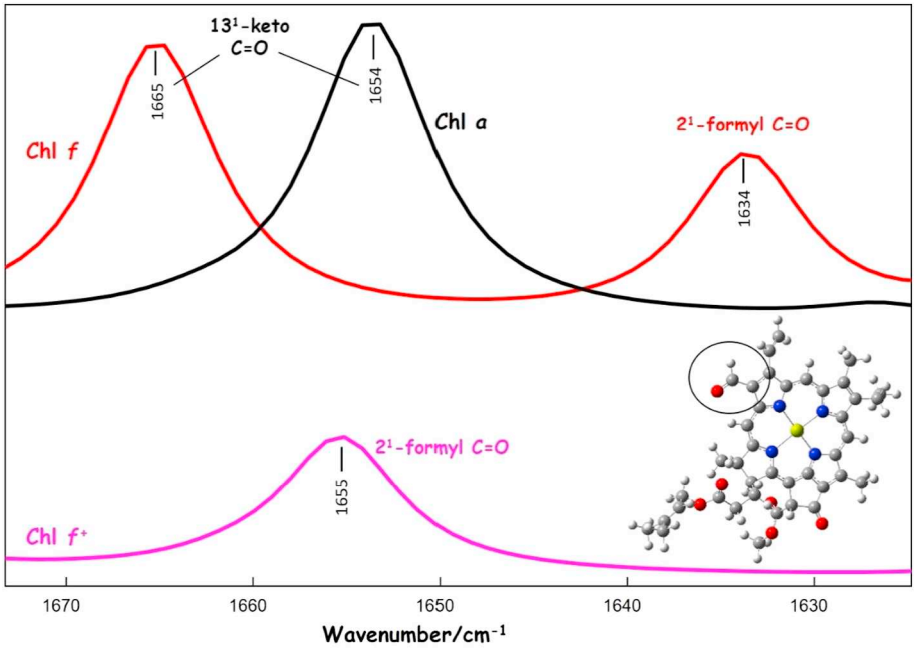

Fig. 6. DFT calculated IR spectra of Chl *a* (*black*), Chl *f* (*red*) and Chl f^+ (*magenta*) in THF. Frequency scaling factor was 0.989. *Inset*: Optimized molecular model for neutral Chl *f* in THF. Rotating the formyl group (*circled*) by ~180° upshifts the formyl C=O mode frequency ~3 cm^{-1}.

Table 1
Band frequencies of the C=O modes of the P_A and P_B pigments of P700 in WL-PSI.

Molecular group	P700	Molecular Group	$P700^+$
13^3-methylester C=O of P_A	1734(−)	13^3-methylester C=O of P_A^+	1742(+)
13^3-methylester C=O of P_B	1748(−)	13^3-methylester C=O of P_B^+	1754(+)
13^1-keto C=O of P_A	1636(−)	13^1-keto C=O of P_A^+	1653 (+)
13^1-keto C=O of P_B	1698(−)	13^1-keto C=O of P_B^+	1718 (+)

for WL-PSI is upshifted 1–2 cm^{-1} compared to the corresponding band in the FRL-PSI FTIR DS.

The band frequency shifts in the FTIR DS for FRL-PSI and WL-PSI are more easily assessed in the (WL – FRL) FTIR DDS, which is also shown in Fig. 4. The quadruple feature at 1632(−)/1643(+)/1651(+)/1659(−) cm^{-1} in the DDS indicates a ~9 cm^{-1} upshift of a complete difference band on going from WL-PSI to FRL-PSI. The 1636(−)/1653(+) cm^{-1} difference band is due to the H-bonded 13^1-keto C=O group of P_A (Table 1), so the fact that it upshifts completely in FRL-PSI indicates a modification of this H-bond in FRL-PSI, in both the neutral and cation states.

ThrA743 is H-bonded to the 13^1-keto C=O of P_A (Fig. 2) and in mutant PSI particles in which ThrA743 was replaced with a non H-bonding Ala reside, the 1636(−)/1653(+) cm^{-1} difference band was found to upshift 30–35 cm^{-1} [36,37]. Such a mutation-induced shift indicates what to expect for the loss of an H-bond to the 13^1-keto C=O group of P_A, and gives some context from which to consider the extent by which the H-bond has been altered in FRL-PSI, for which only a 9 cm^{-1} shift is observed.

A clear difference band is still observed at 1643(−)/1659(+) cm^{-1} in the FTIR DS for FRL-PSI, and indicates that the 13^1-keto C=O group of P_A is still strongly H-bonded in FRL-PSI but that the strength of the H-bond is weakened. One would therefore expect the amino acids involved in the H-bond network near P_A (SerA607, TyrA603, ThrA743 in Fig. 2), to be conserved in the PsaA proteins in WL-PSI and FRL-PSI. This is indeed found to be the case (Fig. S2).

It is well known that the PsaA and PsaB proteins that bind the P_A and P_B pigments of P700 are considerably different in FRL-PSI [16], so some alterations in the protein environment near the P_A and P_B pigments of P700 could be expected (see Fig. S2 for changes in the vicinity of P_A). Further evidence for an altered protein environment near P700 in FRL-PSI is the observation of a set of features at 1552(+)/1544(−)/1535(+) cm^{-1} in the FTIR DDS in Fig. 4 that are due to amide II protein absorption bands [39]. Amide II absorption bands are due to NH bending modes of the protein backbone [39]. The observation of amide II contributions in the FTIR DDS suggests amide I features may also contribute. Amide I absorption bands are associated with peptide C=O stretching vibrations, and are found most often in the 1660–1645 cm^{-1} region for α-helices [39], and at lower (1630 cm^{-1}) and higher (1690 cm^{-1}) frequencies for parallel and anti-parallel β-sheet structures, respectively [39,40]. The FTIR DDS is quite congested in the 1670–1630 cm^{-1} region, and it is not obvious if any of the observed features can be assigned to amide I protein absorptions. The 1636(−) cm^{-1} band in the WL-PSI FTIR DS displays a weak shoulder on the high frequency side of the band that might indicate amide I absorption.

Most of the other features in the DDS in Fig. 4 are weak, indicating small shifts. To analyze these small shifts in greater detail, FTIR DS were collected at 2-cm^{-1} spectral resolution, and these data are shown in Fig. 5.

At 2-cm^{-1} spectral resolution a clear derivative feature is observed at 1669(−)/1664(+) cm^{-1}. This feature could correspond to changes in an amide I protein vibration, although one might expect such a feature to be closer to ~1650 cm^{-1}. Another possibility is that this difference feature is due to a 2^1-formyl C=O of a Chl *f* molecule that is perturbed (electrostatically) by $P700^+$ formation. Because this formyl group would not be present in WL-PSI, only a single derivative-like feature is expected in the DDS. The (WL - FRL) DDS indicate that the formyl C=O upshifts ~5 cm^{-1} upon $P700^+$ formation, and is ~34 cm^{-1} lower in frequency than the 13^1-keto C=O mode. To assess and understand these suggested shifts, we have undertaken DFT-based harmonic, normal-mode, vibrational frequency calculations for neutral Chl *a* and Chl *f* in THF. We also performed calculations for Chl f^+ in THF. The calculated spectra are shown in Fig. 6.

Four features are noteworthy in Fig. 6: 1) Chl *f* displays an intense band at 1669 cm^{-1} while Chl *a* does not. This band is due to the 2^1-formyl C=O of Chl *f*; 2) For Chl *f*, the band of the 2^1-formyl C=O mode is 31 cm^{-1} lower in frequency than the band of the 13^1-keto C=O; 3) The 13^1-keto C=O band of Chl *f* is 9 cm^{-1} higher in frequency than that found for Chl *a* (what we call the 13^1-keto C=O mode is actually somewhat mixed, containing contributions from the 13^3-methylester C=O group also [28,29]); 4) The calculations predict that a 2^1-formyl C=O group of Chl *f* upshifts 21 cm^{-1} upon cation formation.

Point 2 supports the notion that the 1664(+)/1669(−) cm^{-1} feature in the DDS in Fig. 5 could be due to the 2^1-formyl C=O mode of a Chl *f* pigment. Point 4, that a formyl C=O group of Chl *f* would upshift ~20 cm^{-1} upon cation formation, is much larger than the 5 cm^{-1} shift suggested in the experimental FTIR DDS. These calculated and experimental data together therefore further support the notion that Chl *f* is not one of the pigments of P700. That is, the much smaller observed shift indicates that the Chl *f* molecule is more likely to be impacted electrostatically by a charged pigment, but is unlikely to be a charged pigment itself.

The observation of a difference band associated with an electrochromically impacted formyl C=O group would further suggest that the Chl *f* molecule that is impacted is close to the P700 pigments. On both the A and B branches, the A_{-1} and A_0 pigments are ~12 and 19 Å from either P_B or P_A (Mg…Mg distance) (Table S1, Fig. 1B) [4]. However, on both branches, the 2^1 carbon atom of the A_{-1} and A_0 pigments are at a similar distance from the P_A or P_B pigments (Table S1), so it is difficult to assess if the Chl *f* molecule giving rise to the band associated with the formyl C=O mode in the FTIR DS is due to A_0 or A_{-1}. A key observation, however, is that, on both branches, the 13^1-keto C=O oxygen atom of A_{-1} is ~6 Å from P_B or P_A, while the 13^1-keto C=O oxygen atom of A_0 is ~25 Å from P_B or P_A (Table S1). Similarly, the 13^3-methylester C=O group of A_{-1} is much closer to the pigments of P700 than the corresponding group of A_0 (Table S1). These observations, along with the discussion below of bands in the FTIR DS associated with the 13^1-keto and 13^3-methylester C=O groups, lead us to assign the band associated with the 2^1-formyl C=O mode in the FTIR DS with a Chl *f* molecule occupying the A_{-1} binding site.

A Chl *a* molecule functions as the primary electron acceptor in all known homodimeric and heterodimeric type-1 RCs [41], and the data presented here for FRL-PSI are in agreement with, and strengthen, this observation.

The FTIR DS appear to indicate only one band that could be assigned to a formyl C=O group, suggesting that only one Chl *f* molecule is present near either the P_A or P_B pigments. The visible DS (Fig. 3) on the other hand might suggest two Chl *f* bands at ~750 and ~780 nm. It might be possible that a small part of the 1659(−)/1651(+) cm^{-1} feature in the DDS in Fig. 5 is also associated with a formyl C=O group, and hence the FTIR DS might be compatible with contributions from two Chl *f* pigments near the P700 pigments, acting as the A_{-1A} and A_{-1B} cofactors. Further studies at low temperature may help in elucidating if two Chl *f* molecules are near the P700 pigments.

At present, the data unambiguously supports the idea that at least one Chl *f* molecule is in sufficiently close proximity to one of the P700 pigments to be electrostatically affected by the charge on $P700^+$. If the charge is evenly distributed over the P700 pigments, as has been suggested from FTIR data [35], then the Chl *f* molecule could be on either the A or B branch. If the charge over the pigments of P700 is mostly on the B branch, as has been suggested by EPR data [38,42], then the electrostatically affected A_{-1} Chl *f* molecule would most likely be on the B branch.

The FTIR DDS in Fig. 5 indicates an intense difference feature at 1702(+)/1696(−) cm^{-1}. Given the frequency, this feature is most likely associated with 13^1-keto C=O modes of Chl *a* and/or *f*. The calculated spectra in Fig. 6 provides a clue as they indicate that the 13^1-keto C=O mode of Chl *f* is ~9 cm^{-1} higher than for Chl *a*. Thus, we can associate the 1696(−)/1702(+) cm^{-1} feature with neutral Chl *a*/*f* molecules that act as A_{-1} in WL/FRL PSI, respectively. The 13^1-keto C=O mode of the A_{-1} Chl *f* molecule in FRL-PSI is at 1702 cm^{-1}, which is 6 cm^{-1} higher than for the corresponding mode of the A_{-1} Chl *a* molecule in WL-PSI.

The 1696(−) cm^{-1} feature in the DDS in Fig. 5 is relatively intense, and makes a considerable contribution to the 1698(−) cm^{-1} difference band in the FTIR DS for WL PSI. Such a large intensity contribution to the 1698(−) cm^{-1} band suggest a very strong electrochromism, which in turn suggests that the 13^1-keto C=O mode(s) responsible for the 1696(−) cm^{-1} feature in the DDS be very close to the charge on $P700^+$. Again, the 13^1-keto C=O oxygen atom of A_{-1} is much closer to P than the 13^1-keto C=O oxygen atom of A_0 (~6 Å as opposed to ~25 Å (Table S1)). Therefore, we conclude that the 13^1-keto C=O group of at least one of the A_{-1} Chl *a* molecules in WL-PSI gives rise to a band at 1696 cm^{-1}, and is replaced by a Chl *f* molecule in FRL-PSI giving a band at 1702 cm^{-1}. These assignments are in agreement with the calculated spectra in Fig. 6.

Given the above assignments the question of whether the charge on $P700^+$ would induce an upshift or a downshift of the bands associated with the 13^1-keto C=O group of the A_{-1} pigments arises. From the data in Fig. 5 one possibility could be that the 1696(−) cm^{-1} feature in the DDS downshifts 10 cm^{-1}, giving rise to a positive feature observed at 1686 cm^{-1} in the DDS. However, such an interpretation also suggests that the 1702(+) cm^{-1} feature in the DDS downshift to ~1693 cm^{-1}, giving rise to a negative feature in the DDS. A negative feature at ~1693 cm^{-1} would overlap with other negative features already considered, making it difficult to draw any firm conclusions.

The emerging interpretation indicates that the broad 1698 cm^{-1} band in WL-PSI FTIR DS contains a contribution (at 1696 cm^{-1}) from the 13^1-keto C=O mode of the A_{-1} Chl *a* molecule, which could downshift to 1687 cm^{-1} upon cation formation. Such an interpretation could help explain the presence of the 1687 cm^{-1} band in ($P700^+$ – P700) FTIR DS, which up to this point has never been explained. Such an interpretation could also help explain the splitting of the 1698(−) cm^{-1} band observed in ($P700^+$ – P700) FTIR DS that have been obtained using site-directed mutant PSI particles in which the axial histidine ligand to P_A has been changed to serine [8].

The difference feature at 1702(+)/1696(−) cm^{-1} could also be due to a 6 cm^{-1} upshift in the 13^1-keto C=O mode of the P_B pigment of P700 in FRL-PSI, that is caused by an altered protein environment around P_B. We disfavor this hypothesis because the P_B pigment is relatively free from protein interactions (Fig. 2) that would have to disappear or be considerably altered in order to give rise to such a shift in FTIR DS for FRL-PSI.

If the 13^1-keto C=O of A_{-1} is upshifted because of the A_{-1} pigment changing from Chl *a* to Chl *f* in FRL-PSI, then one might also expect changes in the 13^3-methylester C=O spectral region, and the difference feature at 1754(+)/1750(−) cm^{-1} in the DDS supports this idea.

In a similar manner to that outlined above for bands associated with the 13^1-keto C=O of A_{-1}, we associate the 1754(+)/1750(−) cm^{-1} difference features in the DDS with the 13^3-methylester C=O modes of Chl *f*/Chl *a* in the A_{-1} binding site in in WL/FRL PSI, respectively. The 13^3-ester C=O mode of the A_{-1} Chl *f* molecule in FRL-PSI is therefore 4 cm^{-1} higher than for the corresponding mode of the A_{-1} Chl *a* molecule in WL-PSI. Furthermore, the 13^3-ester C=O modes of the A_{-1} Chl *a* and *f* molecules could both downshift ~4 cm^{-1} upon $P700^+$ formation. This would then explain the positive feature at 1745(+) cm^{-1} in the DDS, which would be due to the 13^3-methylester C=O mode of the A_{-1} Chl *a* in WL-PSI, in the presence of $P700^+$. The 13^3-methylester C=O mode of Chl *f* in FRL-PSI in the presence of $P700^+$ would then give rise to a negative feature near 1750 cm^{-1} in the DDS, overlapping other negative features at this wavelength. The multiple overlapping negative features near 1750 cm^{-1} could explain the increased intensity of this band (relative to the 1754(+) cm^{-1} band) in the DDS.

Contributions from 13^3-methylester C=O bands of A_{-1} pigments to ($P700^+$ – P700) FTIR DS could help explain some previously puzzling

results obtained from FTIR studies of PSI particles in which the 13^4-methyl hydrogen atoms of all Chl *a* molecules had been specifically deuterated [14]. In that study multiple difference features in ($P700^+$ – P700) FTIR DS, in the 1760–1690 cm^{-1} region, were interpreted to indicate that the 13^3-methylester C═O of three or more different Chl *a* molecules contributed to ($P700^+$ – P700) FTIR DS. This work was undertaken prior to the widespread availability of a high-resolution PSI crystal structure, and the possibility of electrochromic effects caused by the positive charge of $P700^+$ on nearby A_{-1} Chl *a* pigments were not considered.

Shifts of spectral bands in response to nearby charged pigments plays a prominent role in the interpretation of the DS in this manuscript. This is not unexpected, as such shifts/features are often observed in both visible and infrared difference spectra. For example, the positive band (or peak) near 690 nm in ($P700^+$ – P700) DS has long been considered to be partly due to an electrochromic effect on a pigment near $P700^+$ [43,44], likely the A_{-1} pigment. In FTIR DS studies of purple bacterial reaction centers, bands associated with the 13^3-methylester C═O of the bacteriopheophytin ET cofactor have been observed to shift in response to a negative charge on the quinone occupying the Q_A binding site [45,46]. In this case the distance between relevant cofactor atoms is ~8–9 Å, considerably larger than the distances considered in this manuscript (Table S1). Finally, in time-resolved FTIR DS studies of cyanobacterial PSI, the charge on A_1^- has been proposed to induce a shift of a band associated with the 13^3-methylester C═O of A_0 [47]. In this case the distance between relevant atoms is ~7–8 Å.

Transparency document

The Transparency document associated with this article can be found, in online version.

Acknowledgments

GH acknowledges support from the Department of Energy (DE-SC0017937). DAB acknowledges support from the National Science Foundation (MCB–1613022). GH also acknowledges the use of Georgia State's research computing resources that are supported by Georgia State's Research Solutions, and Peter Walker for expert technical help. The statements made herein are solely the responsibility of the authors.

Appendix A. Supplementary data

Supplementary data to this article can be found online at https://doi.org/10.1016/j.dummy.2019.01.002.

References

[1] D. Walker, Energy, plants and man, Brighton, East Sussex: Mill Valley, 2nd ed., Oxygraphics, CA, 1993.
[2] J. Golbeck, Photosystem I the light driven plastocyanin:ferridoxin oxidoreductase, Advances in Photosynthesis and Respiration, vol. 24, Springer, Dordrecht, 2006.
[3] J. Golbeck, D. Bryant, Photosystem I, Current Topics in Bioenergetics, Academic Press, New York, 1991, pp. 83–175.
[4] P. Jordan, et al., Three-dimensional structure of cyanobacterial photosystem I at 2.5 angstrom resolution, Nature 411 (6840) (2001) 909–917.
[5] K. Brettel, Electron transfer and arrangement of the redox cofactors in photosystem I, Biochim. Biophys. Acta 1318 (3) (1997) 322–373.
[6] I.R. Vassiliev, et al., Near-IR absorbance changes and electrogenic reactions in the microsecond-to-second time domain in photosystem I, Biophys. J. 72 (1) (1997) 301–315.
[7] J. Breton, J. Golbeck (Ed.), FTIR Studies of the Primary Electron Donor, P700, in Photosystem I: The Light Driven Plastocyanin:Ferredoxin Oxidoreductase, Springer, Dordrecht, 2006, pp. 271–289.
[8] G. Hastings, et al., Primary donor photo-oxidation in photosystem I: a re-evaluation of ($P700^+$ - P700) Fourier transform infrared difference spectra, Biochem. 40 (43) (2001) 12943–12949.
[9] J. Breton, Fourier transform infrared spectroscopy of primary electron donors in type I photosynthetic reaction centers, Biochim. Biophys. Acta 1507 (1–3) (2001) 180–193.
[10] G. Hastings, Time-resolved step-scan Fourier transform infrared and visible absorption difference spectroscopy for the study of photosystem I, Appl. Spectrosc. 55 (7) (2001) 894–900.
[11] J. Breton, P.R. Chitnis, M. Pantelidou, Evidence for hydrogen bond formation to the PsaB chlorophyll of P700 in photosystem I mutants of *Synechocystis* sp. PCC 6803, Biochemistry 44 (14) (2005) 5402–5408.
[12] J. Breton, et al., The two histidine axial ligands of the primary electron donor chlorophylls (P700) in photosystem I are similarly perturbed upon $P700^+$ formation, Biochemistry 41 (37) (2002) 11200–11210.
[13] R.L. Wang, et al., FTIR difference spectroscopy in combination with isotope labeling for identification of the carbonyl modes of P700 and P700(+) in photosystem I, Biophys. J. 86 (2) (2004) 1061–1073.
[14] S. Kim, B.A. Barry, Identification of carbonyl modes of P-700 and P-700(+) by in situ chlorophyll labeling in photosystem I, J. Am. Chem. Soc. 122 (20) (2000) 4980–4981.
[15] M. Chen, et al., A red-shifted chlorophyll, Science 329 (5997) (2010) 1318–1319.
[16] F. Gan, et al., Extensive remodeling of a cyanobacterial photosynthetic apparatus in far-red light, Science 345 (6202) (2014) 1312–1317.
[17] M.Y. Ho, et al., Light-dependent chlorophyll *f* synthase is a highly divergent paralog of PsbA of photosystem II, Science 353 (6302) (2016).
[18] C. Zhao, et al., RfpA, RfpB, and RfpC are the master control elements of Far-Red Light Photoacclimation (FaRLiP), Front. Microbiol. 6 (1303) (2015).
[19] F. Gan, G. Shen, D. Bryant, Occurrence of Far-Red Light Photoacclimation (FaRLiP) in diverse cyanobacteria, Life 5 (1) (2015) 4–24.
[20] D.J. Nürnberg, et al., Photochemistry beyond the red limit in chlorophyll f–containing photosystems, Science 360 (6394) (2018) 1210–1213.
[21] V. Kurashov, et al., Energy transfer from chlorophyll *f* to the trapping center in naturally occurring and engineered Photosystem I complexes, Photosynth. Res. (2019), https://doi.org/10.1007/s11120-019-00616-x (In press).
[22] Y. Li, N. Vella, M. Chen, Characterization of isolated photosystem I from *Halomicronema hongdechloris*, a chlorophyll *f*-producing cyanobacterium, Photosynthetica 56 (1) (2018) 306–315.
[23] R. Rippka, et al., Generic assignments, strain histories and properties of pure cultures of cyanobacteria, Microbiology 111 (1) (1979) 1–61.
[24] J.M. Dubbs, D.A. Bryant, Molecular cloning and transcriptional analysis of the *cpeBA* operon of the cyanobacterium *Pseudanabaena* species PCC 7409, Mol. Microbiol. 5 (12) (1991) 3073–3085.
[25] G. Shen, et al., Characterization of chlorophyll *f* synthase heterologously produced in *Synechococcus* sp. PCC 7002, Photosynth. Res. 140 (2019) 77–92.
[26] G. Shen, et al., Assembly of photosystem I. I. Inactivation of the *rubA* gene encoding a membrane-associated rubredoxin in the cyanobacterium *Synechococcus* sp. PCC 7002 causes a loss of photosystem I activity, J. Biol. Chem. 277 (23) (2002) 20343–20354.
[27] M.J. Frisch, et al., Gaussian 16 Rev. B.01, (2016) (Wallingford, CT).
[28] R. Wang, S. Parameswaran, G. Hastings, Density functional theory based calculations of the vibrational properties of chlorophyll *a*, Vib. Spectrosc. 44 (2007) 357–368.
[29] S. Parameswaran, R.L. Wang, G. Hastings, Calculation of the vibrational properties of chlorophyll *a* in solution, J. Phys. Chem. B 112 (44) (2008) 14056–14062.
[30] J. Tomasi, et al., Molecular properties in solution described with a continuum solvation model, Phys. Chem. Chem. Phys. 4 (23) (2002) 5697–5712.
[31] J. Tomasi, B. Mennucci, R. Cammi, Quantum mechanical continuum solvation models, Chem. Rev. 105 (8) (2005) 2999–3093.
[32] J. Tomasi, B. Mennucci, E. Cances, The IEF version of the PCM solvation method: an overview of a new method addressed to study molecular solutes at the QM ab initio level, J. Mol. Struct. (THEOCHEM) 464 (1–3) (1999) 211–226.
[33] E. Cances, B. Mennucci, J. Tomasi, A new integral equation formalism for the polarizable continuum model: theoretical background and applications to isotropic and anisotropic dielectrics, J. Chem. Phys. 107 (8) (1997) 3032–3041.
[34] H. Witt, et al., Species-specific differences of the spectroscopic properties of P700 - analysis of the influence of non-conserved amino acid residues by site-directed mutagenesis of photosystem I from *Chlamydomonas reinhardtii*, J. Biol. Chem. 278 (47) (2003) 46760–46771.
[35] J. Breton, E. Nabedryk, W. Leibl, FTIR study of the primary electron donor of photosystem I (P700) revealing delocalization of the charge in P700(+) and localization of the triplet character in (3)P700, Biochem. 38 (36) (1999) 11585–11592.
[36] M. Pantelidou, P.R. Chitnis, J. Breton, FTIR spectroscopy of *Synechocystis* 6803 mutants affected on the hydrogen bonds to the carbonyl groups of the PsaA chlorophyll of P700 supports an extensive delocalization of the charge in P700+, Biochemistry 43 (26) (2004) 8380–8390.
[37] H. Witt, et al., Hydrogen bonding to P700: site-directed mutagenesis of threonine A739 of photosystem I in *Chlamydomonas reinhardtii*, Biochemistry 41 (27) (2002) 8557–8569.
[38] W. Lubitz, EPR studies of the primary electron donor P700 in photosystem I, in: J. Golbeck (Ed.), Photosystem I: The Light Driven Plastocyanin:Ferredoxin Oxidoreductase, Springer, 2006, pp. 245–269.
[39] W. Surewicz, H. Mantsch, Infrared absorption methods for examining protein structure, in: H. Havel (Ed.), Spectroscopic methods for Determining Protein Structure in Solution, VCH, New York, N.Y, 1996, pp. 135–162.
[40] H. Susi, D.M. Byler, Resolution-enhanced Fourier transform infrared spectroscopy of enzymes, Methods Enzymol. 130 (1986) 290–311.
[41] J.C. Zill, et al., N-15 photo-CIDNP MAS NMR analysis of reaction centers of *Chloracidobacterium thermophilum*, Photosynth. Res. 137 (2) (2018) 295–305.
[42] A.N. Webber, W. Lubitz, P700: the primary electron donor of photosystem I, Biochim. Biophys. Acta 1507 (1–3) (2001) 61–79.
[43] H. Schaffernicht, W. Junge, Deconvolution of the Red P700 difference spectrum

based on a set of three Gaussian components: further evidence from literature spectra, Photochem. Photobiol. 36 (1) (1982) 111–115.
[44] H. Schaffernicht, W. Junge, Analysis of the complex band spectrum of P700 based on photoselection studies with photosystem I particles, Photochem. Photobiol. 34 (2) (1981) 223–232.
[45] J. Breton, et al., Conformational heterogeneity of the bacteriopheophytin electron acceptor H_A in reaction centers from *Rhodopseudomonas viridis* revealed by Fourier transform infrared spectroscopy and site-directed mutagenesis, Biochemistry 38 (35) (1999) 11541–11552.
[46] J. Breton, et al., Electrostatic influence of Q_A reduction on the IR vibrational mode of the 10a-Ester CO of H_A demonstrated by mutations at residues Glu L104 and Trp L100 in reaction centers from *Rhodobacter sphaeroides*, Biochemistry 36 (15) (1997) 4515–4525.
[47] G. Hastings, FTIR studies of the intermediate electron acceptor A1, in: J. Golbeck (Ed.), Photosystem I: The Light Driven Plastocyanin:Ferredoxin Oxidoreductase, Springer, Dordrecht, 2006, pp. 301–318.